Ultrasonics Sonochemistry 19 (2012) 701–706

Contents lists available at SciVerse ScienceDirect

Ultrasonics Sonochemistry

journal homepage: www.elsevier.com/locate/ultsonch

Effect of ultrasound on the kinetics of cation exchange in NaX zeolite

Yasemin Erten-Kaya *, Fehime Cakicioglu-Ozkan

Izmir Institute of Technology, Department of Chemical Engineering, Urla, İzmir, Turkey

ARTICLE INFO

Article history:
Received 10 August 2011
Received in revised form 14 October 2011
Accepted 14 October 2011
Available online 25 October 2011

Keywords:
NaX zeolite
Ultrasound
Ion exchange
Kinetics

ABSTRACT

In this study, we focused on the effect of ultrasound on ion exchange kinetics to obtain the Li-, Ca- and Ce-rich NaX zeolite. The results were compared to those obtained from the traditional batch exchange method under similar conditions. Contact time and initial cation concentration (fold equivalent excess) were studied. Ultrasound enhanced the replacement of Na^+ ion with Li^+, Ca^{2+} and Ce^{3+} ions in the extra-framework of zeolite up to 76%, 72% and 66%, respectively. The intraparticle diffusion is the rate limiting step in the ion exchange for both exchange methods. As compared to the traditional exchange method, the ultrasonic method applied in this study was found to be very effective on the exchange amount at equilibrium.

1. Introduction

NaX zeolite, a porous crystalline aluminosilicate has three dimensional open frameworks consisting of AlO_4 and SiO_4 tetrahedra linked to each other by sharing the oxygen. The framework is composed by linking sodalite cages (sodalite cavity) through double six-rings (D6R) which create a large cavity called the "supercage" accessible by a three-dimensional 12-ring pore system (Fig. 1). The framework bears negative charges on AlO_4 tetrahedron balanced by an extra-framework of cations such as alkaline or alkaline earth ions. These cations are mobile and undergo ion exchange [1,2].

Extra-framework cations have their principle sites in the unit cell of X type zeolite structure. Site I (SI) is in the center of the hexagonal prism, while site II (SII) and site III (SIII) are in the single six-membered ring (S6R) and near the four-ring windows of the supercage [3]. These cations were exchanged with counter ions which prefer to locate themselves at different sites in the unit cell of NaX zeolite. According to the literature, Li^+ ions occupy the plane of the six-membered ring, preferentially the SI′ and SII and when the exchange degree is 80%, SIII. Ce^{3+} ions are least stable in SII and Ca^{2+} ions initially prefer to locate SI and SI′ in NaX zeolite as stated by Jasra et al. [4]. The location of cations determines the application field of zeolite in industry.

Ultrasound is a source of high energy vibrations that produces mechanical waves with frequencies above the human hearing upper limit (18 kHz). The sonochemistry (frequency range: 20 kHz–2 MHz), power (frequency range: 20–100 kHz) and diagnostic (frequency range: 5 MHz–1 GHz) ultrasound are three strands of the ultrasound. The first one is used for synthesis, catalysis, improved extraction, crystallization, modification of enzyme and so on. The use of the second one includes cleaning, welding and material processing. The last one is used for non-destructive testing and medical scanning [5]. The acoustic wave, by ultrasonic irradiation, creates micro bubbles. The collapse of millions of bubbles (or cavities) which generates cavitations, is a rapid formation and origin of the ultrasonic effect. Implosive collapse of these bubbles caused high speed microjets (400 km h^{-1}) to immerse and high pressure shock waves on or near adsorbent surface [5]. Another possible physical process mechanism of ultrasound is the acoustic streaming or steady flow, the movement of the liquid promoted by acoustic wave without cavitation. These process mechanisms are very effective for reducing the boundary layer thickness below 1 μm and can result in mass transfer enhancement [6].

In recent years, several studies have been made to report the effect of ultrasound on the mass transfer mechanisms: bulk diffusion, external diffusion, intraparticle diffusion. In these studies, ultrasound was generated by using the horn or ultrasonic cleaner. Rege et al. [7] studied desorption of phenol from activated carbon and polymeric resin adsorbents using ultrasonic horn. Mechanism of desorption was altered with the application of the ultrasound at 40 kHz and 1.44 MHz. They found that phenol desorption rates were enhanced with the ultrasound due to an increase in diffusive transport within the pores. In another study, the effect of ultrasound was investigated on the leaching process [8,9]; Geniposide leaching from the Gardenia fruit. Ultrasound increased the external mass transfer and intraparticle diffusion coefficients. In the degradation of the acetic acid, Fındık et al. [10] investigated the effect of the frequency and power range of the ultrasound to minimize the

* Corresponding author. Tel.: +90 2327506677; fax: +90 2327506645.
E-mail address: yaseminerten@iyte.edu.tr (Y. Erten-Kaya).

1350-4177/$ - see front matter © 2011 Elsevier B.V. All rights reserved.
doi:10.1016/j.ultsonch.2011.10.010

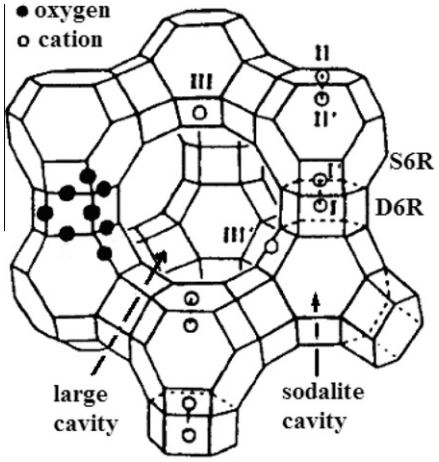

Fig. 1. Unit cell structure of NaX zeolite with cation sites (I, I′, II, II′, III, III′).

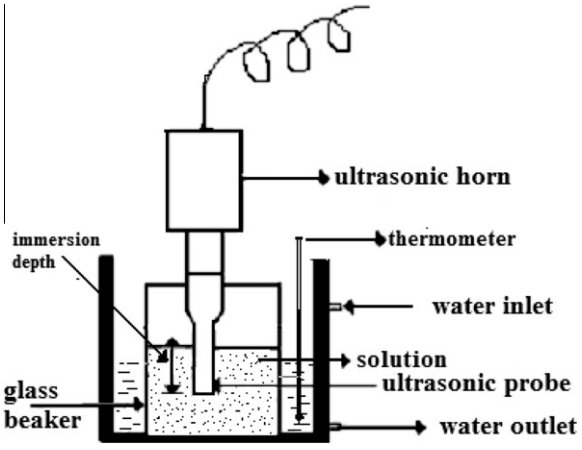

Fig. 2. Experimental set-up of ultrasonic probe.

energy requirement for treatment. In the synthesis of nano-sized $LiCoO_2$ powders [11], ultrasound was found very effective compared to the hydrothermal synthesis and refluxing methods with respect to reaction time and phase purity. Ultrasound has been applied successfully to leaching, desorption, degradation reaction, however the mechanism in these applications is not yet clear.

The goal of this work is to investigate the effect of ultrasonic cavitation on the sodium replacement kinetics in 13X zeolite under different initial counter ion (Li^+, Ca^{2+}, Ce^{3+}) concentrations.

2. Experimental

Commercial NaX zeolite (13X) in the crystal size of 2 μm was used in binderless form (Aldrich). Cerium ($CeCl_3{\cdot}7H_2O$), calcium ($CaCl_2{\cdot}2H_2O$) and lithium (LiCl) salts with high purity of 99.6%, 99–102% and 99%, respectively, were used in ion exchange experiment.

The experimental conditions used in the ion exchange were presented in Table 1. The exchange solutions were centrifuged (Rotofix 32, Hettich) and then washed several times to obtain the zeolites Cl^- free.

The ultrasound processor (Sonics-Vibra Cell 505) with 20 ± 0.050 kHz frequency and 25% of acoustic power (500 W) were used in the experiments. The processor has the replaceable probe tip having 1/2 in. (13 mm) diameter. The probe was dipped to a depth of 15 mm and the temperature of the solution sonicated was maintained at 70 °C with circulating water (Fig. 2). Traditional batch ion exchange experiments were performed in the water bath shaker (GFL 1092) at 70 °C and 130 rpm. All experiments were provided for a sufficient time to enable the system to approach equilibrium. The experiments were repeated at least two times and mean values were taken. Inductively Coupled Plasma Atomic Emission Spectroscopy (ICP-AES 96, Varian) was used to determine the cation content of the aqueous solution centrifuged.

In the code of the solutions, the numbers (3, 5, 6 or 9) and the following letters (T for traditional and U for ultrasonic) were used for the fold equivalent excess and the exchange methods, respectively.

Table 1
Experimental conditions of the ion exchange experiment.

Solution	Concentrations (M)	pH	Fold equivalent excess
LiCl	2	7.2 ± 0.5	3, 6, 9
$CaCl_2{\cdot}2H_2O$	2	5.7 ± 0.25	3, 6, 9
$CeCl_3{\cdot}7H_2O$	0.08	5.5 ± 0.25	3, 5, 6, 9

3. Results and discussion

The ion exchange performed in this study;

$$M^{z+}_{(aq)} - Na\text{-}X_{(zeo)} \overset{K}{\leftrightarrow} zNa^{+}_{(aq)} + M\text{-}X_{(zeo)}$$

where M^{z+} is the counter ions, namely Li^+, Ca^{2+} or Ce^{3+}, K is the rate constant of the ion exchange reaction defined as the ratio of rate of forward to that of reverse reaction. Assuming that counter ions were exchanged with only Na^+ ions into zeolite, the equivalent amount of counter ions in zeolites was calculated. As seen from the kinetic curves of Li^+, Ca^{2+} and Ce^{3+} ion exchange (Figs. 3–5, respectively), the initial rate of exchange was very fast and thereafter it slowed down. Comparison of the exchange methods shows that the time to reach equilibrium in the traditional method is shorter than that in the ultrasonic one. Ultrasound also enhanced the exchange amount by means of transient cavitation bubbles which are found not only in the fluid phase surrounding the particles but also in the solution within the porous particles, compared to the traditional method [8,9].

The effect of the fold equivalent excess of Li^+ and Ca^{2+} ion exchanges is also clearly seen: the higher the amount of the ions present in the solution, the higher the exchange amount. In case of Ce^{3+} ion exchange, the methods applied have a different effect; the exchange amount at equilibrium decreased with increasing excess amount of Ce^{3+} ions in the solution when ultrasonic method was used, whereas it increased in case of the traditional method. However the difference between the methods disappeared at 9-fold equivalent excess. As stated in the literature, cerium is a lanthanide element and has a tendency to hydrolyze with increasing concentration which prevents Ce^{3+} ions to enter the zeolite framework [12]. As a result, ultrasonic method may have accelerated the hydrolysis of Ce^{3+} after the 5-fold equivalent excess compared to the traditional method.

The kinetic models, pseudo second order reaction, intraparticle and external diffusion, were studied to identify the effect of ultrasound on the mass transfer mechanism. The data fitted with the models by decreasing the sum of square of error, SSE:

$$\mathrm{SSE} = \sum \left[\frac{(q - q_{\mathrm{theo}})^2}{q^2} \right] \quad (1)$$

where q and q_{theo} are the experimental and theoretical amount of counter ions in zeolite, respectively. The model parameters obtained are presented in Table 2.

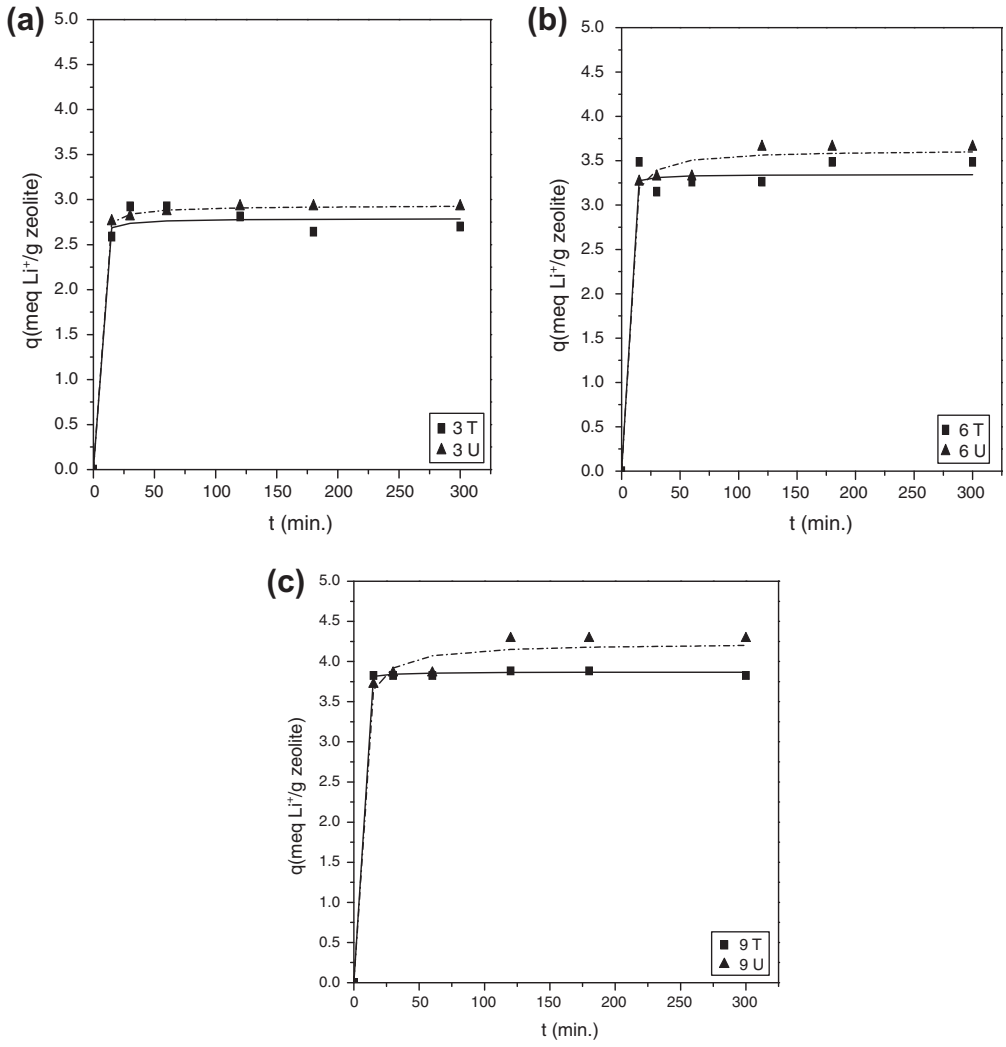

Fig. 3. Kinetic curve of Li^+ exchange with fold equivalent excess; (a) 3, (b) 6, (c) 9; model: second order reaction equation (line), experiments: points.

3.1. Pseudo second order reaction model

The pseudo second order reaction model is used for solid–liquid systems to provide the ion exchange capacity, rate constant and the initial rate of ion exchange [13]. According to the model, the differential change in counter ions of the zeolite:

$$\frac{dq}{dt} = k(q_e - q)^2 \tag{2}$$

where k is the rate constant of pseudo second order reaction (g mequiv.$^{-1}$ min^{-1}), q and q_e (mequiv. g^{-1}) are the amount of the counter ions (Li^+, Ca^{2+} or Ce^{3+}) in the zeolite at any time, t and at equilibrium, respectively. The integration of differential equation (2) by using the initial condition; $q = 0$ at $t = 0$ gives the amount of counter ions in the zeolite at any time, q;

$$q = \frac{t}{\frac{1}{kq_e^2} + \frac{t}{q_e}} \tag{3}$$

and the initial rate (mequiv. g^{-1} min^{-1}) of exchange, when time goes to zero, h;

$$h = kq_e^2. \tag{4}$$

As seen from Table 2, the experimental data were well correlated with this model ($R^2 > 0.99$). The rate of Li^+ exchange (k, h) increased significantly with the fold equivalent excess when the traditional method was used, whereas it decreased in case of ultrasonic method. On the other hand, the rates of ion exchange of the ions at different charges (Ca^{2+} and Na^+ or Ce^{3+} and Na^+) in zeolite was not clear due to lower contribution of Van der Waals interaction than electrostatic interactions [14]. Thus Ca^{2+} and Ce^{3+} are not preferred since their hydrated radius are higher than monovalent cation Na^+.

On the other hand the equilibrated values (q_e) were increased with fold equivalent excess and valence (and hydrated radius) of counter ions (Li^+ and Ca^{2+}) into the solutions for both exchange methods. Furthermore, ultrasonic method is more effective than the traditional one. This can be explained with the theory of "hot spots" [5]: Hot spots increase the temperature and pressure near the surface of the NaX zeolite causing enhancement in the cation exchange as observed during removal of water hardness [15]. The effect of ultrasonic method on Ce^{3+} exchange was also seen when compared with the traditional one. However, the equilibrated values of Ce^{3+} exchange decreased after five fold equivalent excess of Ce^{3+} ions by using the ultrasonic method. It can be explained with the hydrolysis of Ce^{3+} ions with an increasing excess amount of Ce^{3+} ions in solution under the ultrasonic method which prevents Ce^{3+} ions to enter the zeolite extra-framework.

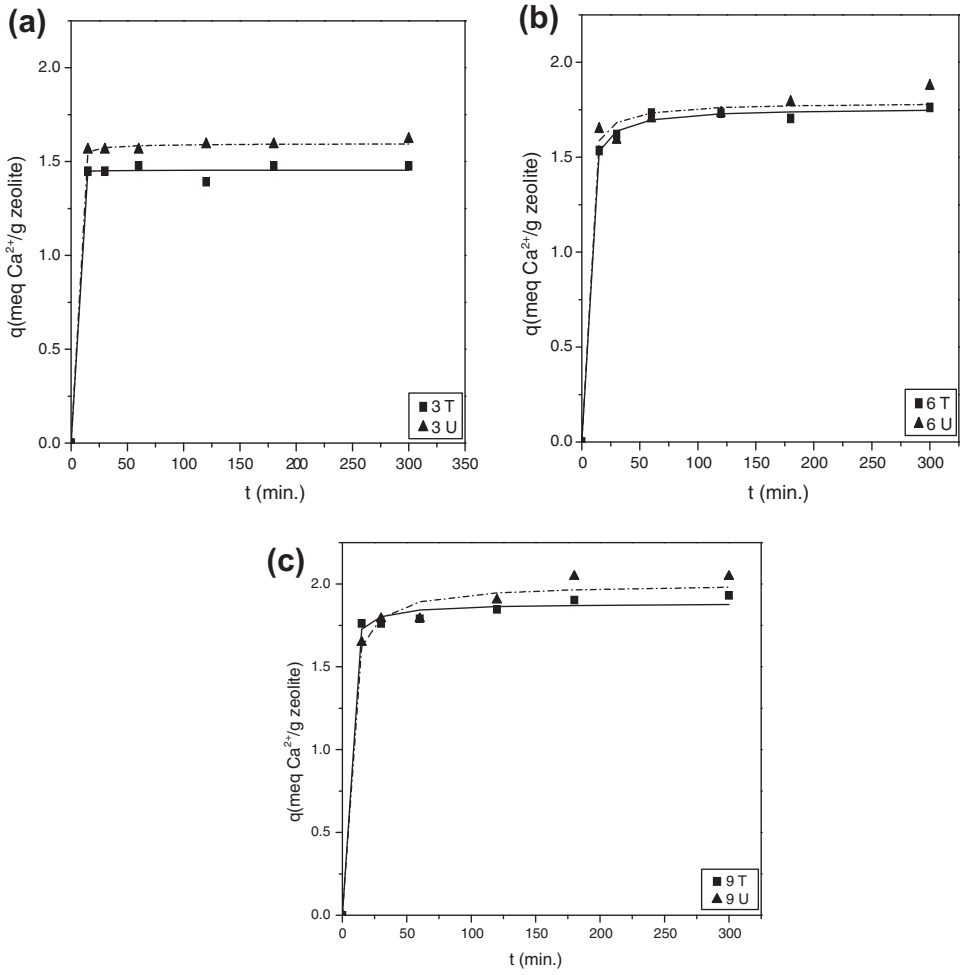

Fig. 4. Kinetic curve of Ca^{2+} exchange with fold equivalent excess; (a) 3, (b) 6, (c) 9; model: second order reaction equation (line), experiments: points.

3.2. Diffusion model: intraparticle and/or external

The differential equation for the diffusion of the counter ions in the spherical particle

$$\frac{dq}{dt} = \frac{1}{r^2}\frac{\partial}{\partial r}\left(r^2 D \frac{\partial q}{\partial r}\right) \tag{5}$$

was solved analytically [16] assuming that initially zeolite is free of counter ions ($q(r, 0) = 0$). The average equivalent amount of counter ions, $\bar{q}$:

$$\frac{\bar{q}}{q_e} = 1 - \frac{6}{\pi^2}\sum_{n=1}^{\infty}\frac{1}{n^2}\exp\left(-\frac{n^2\pi^2 Dt}{r^2}\right) \tag{6}$$

where D ($m^2\ s^{-1}$) is the diffusion coefficient and q_e (mequiv. g^{-1}) is the equivalent amount of counter ions at equilibrium. At the beginning of the exchange the analytic solution Eq. (6) converges to:

$$\frac{\bar{q}}{q_e} = \frac{6}{\sqrt{\pi}}\left(\frac{Dt}{r^2}\right)^{1/2} \quad \text{or} \quad \frac{\bar{q}}{q_e} = k_i t^{1/2} \tag{7}$$

where k_i (mequiv. $g^{-1}\ min^{-1/2}$) is the intraparticle diffusion rate constant. The experimental data collected were fitted to the model by reducing the error ($1 \times 10^{-4} < SSE < 99 \times 10^{-4}$). As seen from Table 2, the conformance of this model is not as good as the reaction model ($0.77 < R^2 < 0.99$). The plot of $\bar{q}/q_e$ versus $t^{1/2}$ did not pass through the origin showing the presence of more than one resistance (intraparticle and/or external film) to the ion exchange [14]. For Li^+ and Ca^{2+} ion exchange, intraparticle diffusion rate constant, k_i, increased significantly with the fold equivalent excess. Due to agglomeration on zeolite surface at high fold equivalent excess which could block the pores and reduce the exchange rate, irregular change in the k_i values for Ce^{3+} exchange was observed. The rate constant of the exchange, k_i, was high when ultrasonic method was used. Comparison of the Li^+ and Ca^{2+} exchange shows that the k_i value decreased with increasing hydrated radius of the ions. The relationship could not be established for Ce^{3+} ions. It can be explained with the cavitation bubbles of ultrasound which collapsed asymmetrically in a heterogeneous system that resulted in micro jet and shockwaves with high velocity on the surface of the zeolite. These actions can lead to reduce the hydrated radius of the Li^+ and Ca^{2+} ions and increase the rate constants as stated by Hamdaoui and Naffrechoux [17].

The intraparticle diffusion coefficient, D, was calculated by using the following modified form of the analytical solution Eq. (6):

$$\frac{q_t}{q_e} = 1 - \frac{6}{\pi^2}\exp\left(-\frac{\pi^2 Dt}{r^2}\right) \tag{8}$$

The collected data fitted with the model by decreasing the SSE values ($3 \times 10^{-4} < SSE < 840 \times 10^{-4}$). The agreement of the data with the model is not better than the previous form of the analytical solution Eq. (7) ($0.58 < R^2 < 0.96$). As seen from Table 2, the intraparticle diffusion coefficient for Li^+ and Ca^{2+} ion exchange increased with decreasing counter ions concentration in the ultrasonic exchange method. The disordered change in diffusion

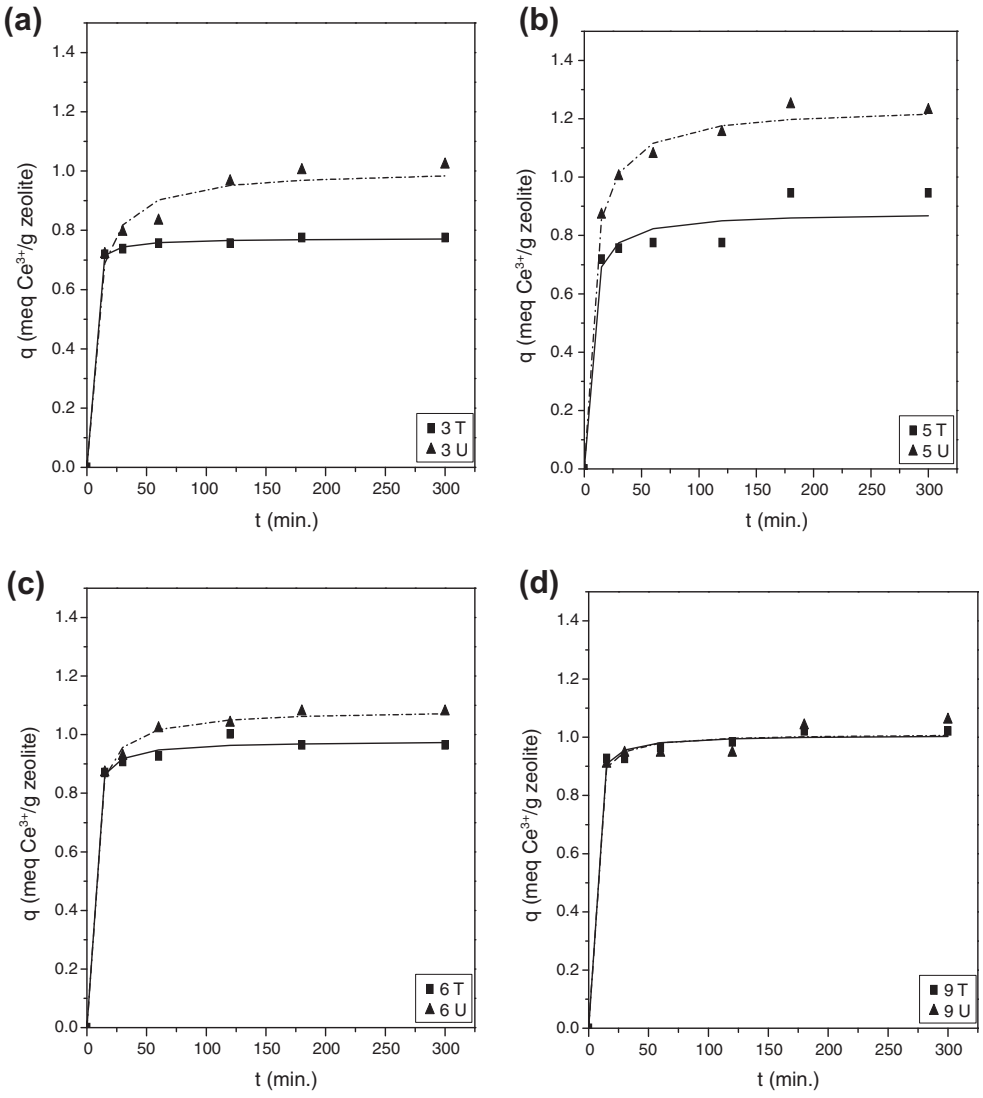

Fig. 5. Kinetic curve of Ce^{3+} exchange with fold equivalent excess; (a) 3, (b) 5, (c) 6, (d) 9; model: second order reaction equation (line), experiments: points.

coefficient with counter ion concentration was observed for Ce^{3+} ion exchange. The effect of hydrated radius of the counter ions on diffusion coefficients was not observed clearly.

The differential change in counter ions in the external film, k_f, was calculated from the mass balance on the spherical particle [18]:

$$\frac{d\bar{q}}{dt} = \frac{3k_f}{Kr}(q_e - \bar{q}) \tag{9}$$

where r is the radius of spherical adsorbent, k_f is the external film mass transfer coefficient ($m\,s^{-1}$), K is the dimensionless Henry's law constant. The experimental data were well correlated with the model ($R^2 > 0.94$) and the SSE values changed from 2×10^{-4} to 824×10^{-4}. As seen from Table 2, the k_f value was changed irregularly with fold equivalent excess and increased with decreasing the valence of the counter ions. The order of the k_f values is;

Li^+ ion exchange $>$ Ca^{2+} ion exchange $>$ Ce^{3+} ion exchange.

To compare the intraparticle resistance to external film resistance, the Biot mass number was calculated:

$$Bi_m = \frac{k_f r_c}{D} \tag{10}$$

where the critical radius, r_c was taken as $r/3$ for sphere. Bi_m values ($0.1 < Bi_m < 0.3$) are not much higher than 0.1 which is the critical value to decide the controlling step in mass transfer. Therefore both intraparticle and external film diffusions are comparable for Li^+, Ca^{2+} and Ce^{3+} ions exchange. However the external film mass transfer seems to be pronounced for multivalent cations rather than monovalent cation.

The unexpected result of the ultrasonic method can rise from insufficient (local) mixing depending on the depth of the tip, shape and type of the beaker used in ion exchange experiment as stated by Klima [6].

4. Conclusion

The effect of the ultrasonic irradiation on the cation (Li^+, Ca^{2+} and Ce^{3+}) exchange was investigated. The change in the mass transfer mechanisms was examined. The external film resistance will decrease with application of the ultrasound if ultrasonic vibration would reduce the thickness of the boundary layer on the surface. However the implosive collapse of bubbles did not accelerate

Table 2
Model parameters of counter ions exchange.

Counter ion[a]	Fold equivalent excess	Pseudo second order reaction model								Diffusion model										Bi_m	
		q_e (mequiv. g^{-1})		k (g mequiv.$^{-1}$ min^{-1})		h (mequiv. g^{-1} min^{-1})		R^2		k_i (mequiv. g^{-1} $min^{-1/2}$)		C		R^2		$D \times 10^{16}$ (m^2 s^{-1})		R^2		$K_f \times 10^{10}$ (m s^{-1})			
		T	U	T	U	T	U	T	U	T	U	T	U	T	U	T	U	T	U	T	U	T	U	T	U
Li^+ (r_H = 3.80)	3	2.79	2.93	0.62	0.33	4.85	2.82	0.9956	0.9999	0.008	0.018	0.95	0.92	0.9719	0.9538	3.02	2.53	0.8660	0.8255	1.3	1.8	0.9990	0.9993	0.2	0.3
	6	3.35	3.63	0.90	0.13	10.0	1.78	0.9940	0.9970	0.014	0.047	0.93	0.83	0.9215	0.9363	0.95	1.67	0.7381	0.6182	0.7	1.3	0.9969	0.9932	0.2	0.2
	9	3.87	4.23	1.15	0.10	17.3	1.76	0.9999	0.9969	0.035	0.085	0.85	0.78	0.9719	0.9425	3.74	0.7	0.6825	0.7604	2.6	1.2	0.9998	0.9923	0.1	0.3
Ca^{2+} (r_H = 4.12)	3	1.45	1.60	10.8	1.48	15.7	3.77	0.9986	0.9997	0.002	0.004	0.97	0.96	0.8001	0.9558	3.72	1.54	0.6999	0.5772	1.2	1.2	0.9998	0.9992	0.1	0.3
	6	1.76	1.79	0.25	0.29	0.78	0.93	0.9994	0.9973	0.011	0.019	0.89	0.82	0.8414	0.9545	1.09	0.69	0.9576	0.7300	0.3	0.3	0.9980	0.9881	0.1	0.2
	9	1.88	2.00	0.38	0.14	1.38	0.56	0.9983	0.9967	0.015	0.030	0.86	0.75	0.9862	0.9518	0.89	0.70	0.7688	0.8622	0.7	0.5	0.9953	0.9889	0.1	0.1
Ce^{3+} (r_H = 9.0)	3	0.77	0.99	1.06	0.16	0.64	0.16	0.9998	0.9940	0.004	0.022	0.91	0.64	0.9199	0.9590	2.24	0.56	0.8314	0.9326	0.4	0.2	0.9989	0.9783	0.1	0.1
	5	0.89	1.24	0.27	0.12	0.21	0.18	0.9907	0.9978	0.018	0.037	0.67	0.54	0.9656	0.9772	0.41	0.64	0.7829	0.9565	0.1	0.2	0.9445	0.9875	0.1	0.1
	6	0.98	1.08	0.51	0.22	0.49	0.27	0.9986	0.9992	0.007	0.016	0.87	0.75	0.7707	0.9030	1.91	1.08	0.8661	0.9361	0.3	0.3	0.9955	0.9939	0.1	0.1
	9	1.00	1.01	0.60	0.50	0.61	0.51	0.9985	0.9951	0.008	0.011	0.86	0.82	0.9602	0.9211	1.82	1.36	0.6662	0.6227	0.4	0.4	0.9955	0.9894	0.1	0.1

[a] r_H: hydrated radius; C: the intercept of the plot relates to the external film resistance.

the exchange of Li^+, Ca^{2+} and Ce^{3+} ions in zeolite due to the point effect of ultrasonic horn. Additionally break down of the crystal with the ultrasound is expected. This did not accelerate the exchange but the equilibrium of the exchange, as will be presented in future articles.

The kinetic of ion exchange data fitted with the pseudo second order reaction and diffusion models. Apart from the external film resistance, the intraparticle diffusion is the rate limiting step in the ion exchange for both exchange methods. The results show that the rate-limiting step of the ion exchange may vary throughout the exchange process and explained into two stages. In the early stage the chemical reaction is dominant and very fast. In the later stage the diffusion process, where the ion exchange slows down, is dominant.

As compared to the traditional exchange method, the ultrasonic method applied in this study was found to be very effective on the exchange amount at equilibrium. Ultrasound acted like a co-driven force of concentration of counter ions in solution due to cavitational effect of ultrasound field and increased the equilibrated values in ion exchange process.

Acknowledgements

The authors wish to thank Izmir Institute of Technology (Project number: 2006IYTE31) and State Planning Organization of Turkey (DPT) for financial support.

References

[1] V.H. Bekkum, E.M. Flanigen, P.A. Jacobs, J.C. Jansen, Introduction Zeolite Science and Practice, second completely revised and expanded ed., Elsevier Science, 2001.
[2] C. Senaratne, M.D. Baker, Zeolite-modified electrodes: electrochemical response as a probe of intracrystalline cation-exchange dynamics in zeolites X and Y, J. Phys. Chem. 98 (1994) 13687–13694.
[3] N.D. Hutson, S.U. Rege, R.T. Yang, Mixed cation zeolites: Li_xAg_y-X as a superior adsorbent for air separation, Separations 45 (1999) 724–734.
[4] R.V. Jasra, N.V. Choundary, S.G.T. Bhat, Correlation of sorption behaviour of nitrogen, oxygen, and argon with cation locations in zeolite X, Ind. Eng. Chem. Res. 35 (1996) 4221–4229.
[5] M.D. Castro, F.P. Capote, Techniques and Instrumentation in Analytical Chemistry: Analytical Applications of Ultrasound, vol. 26, Elsevier BV, 2007.
[6] J. Klima, Application of ultrasound in electrochemistry. An overview of mechanisms and design of experimental arrangement, Ultrasonics 51 (2011) 202–209.
[7] S.U. Rege, R.T. Yang, C.A. Cain, Desorption by ultrasound: phenol on activated carbon and polymeric resin, AIChE J. 44 (1998) 1519–1528.
[8] J. Ji, X. Lu, Z. Xu, Effect of ultrasound on adsorption of geniposide on polymeric resin, Ultrason. Sonochem. 13 (2006) 463–470.
[9] J. Ji, X. Lu, M. Cai, Z. Xu, Improvement of leaching process of geniposide with ultrasound, Ultrason. Sonochem. 13 (2006) 455–462.
[10] B.S. Fındık, G. Gündüz, E. Gündüz, Direct sonication of acetic acid in aqueous solutions, Ultrason. Sonochem. 13 (2006) 203–207.
[11] K.H. Kim, K.B. Kim, Ultrasound assisted synthesis of nano-sized lithium cobalt oxide, Ultrason. Sonochem. 15 (2008) 1019–1025.
[12] H. Faghihian, M.K. Amini, A.R. Nezamzadeh, Cerium uptake by zeolite A synthesized from natural clinoptilolite tuffs, J. Radioanal. Nucl. Chem. 264 (2005) 577–582.
[13] Y.S. Ho, Pseudo-isotherms using a second order kinetic expression constant, Adsorption 10 (2004) 151–158.
[14] Y. Kaya-Erten, The Sorption of N_2, CO_2 and CH_4 on Ultrasound Enhanced Cation Exchanged X Zeolite, Doctoral Thesis, Izmir Institute of Technology, 2011.
[15] M.H. Entezari, M. Tahmasbi, Water softening by combination of ultrasound and ion exchange, Ultrason. Sonochem. 16 (2009) 356–360.
[16] J. Crank, The Mathematics of Diffusion, second ed., Oxford Science Publications, 2003.
[17] O. Hamdaoui, E. Naffrechoux, An investigation of the mechanisms of ultrasonically enhanced desorption, AIChE J. 53 (2007) 363–373.
[18] K. Karger, D.M. Ruthven, Diffusion in Zeolites and Other Microporous Solids, John Wiley and Sons Inc., New York, 2008.